Optical modulation of cell nucleus penetration and singlet oxygen release of a switchable platinum complex

Zakaria Ziani, Saioa Cobo, Nathalie Berthet, Guy Royal

iScience

CellPress
OPEN ACCESS

Article

Optical modulation of cell nucleus penetration and singlet oxygen release of a switchable platinum complex

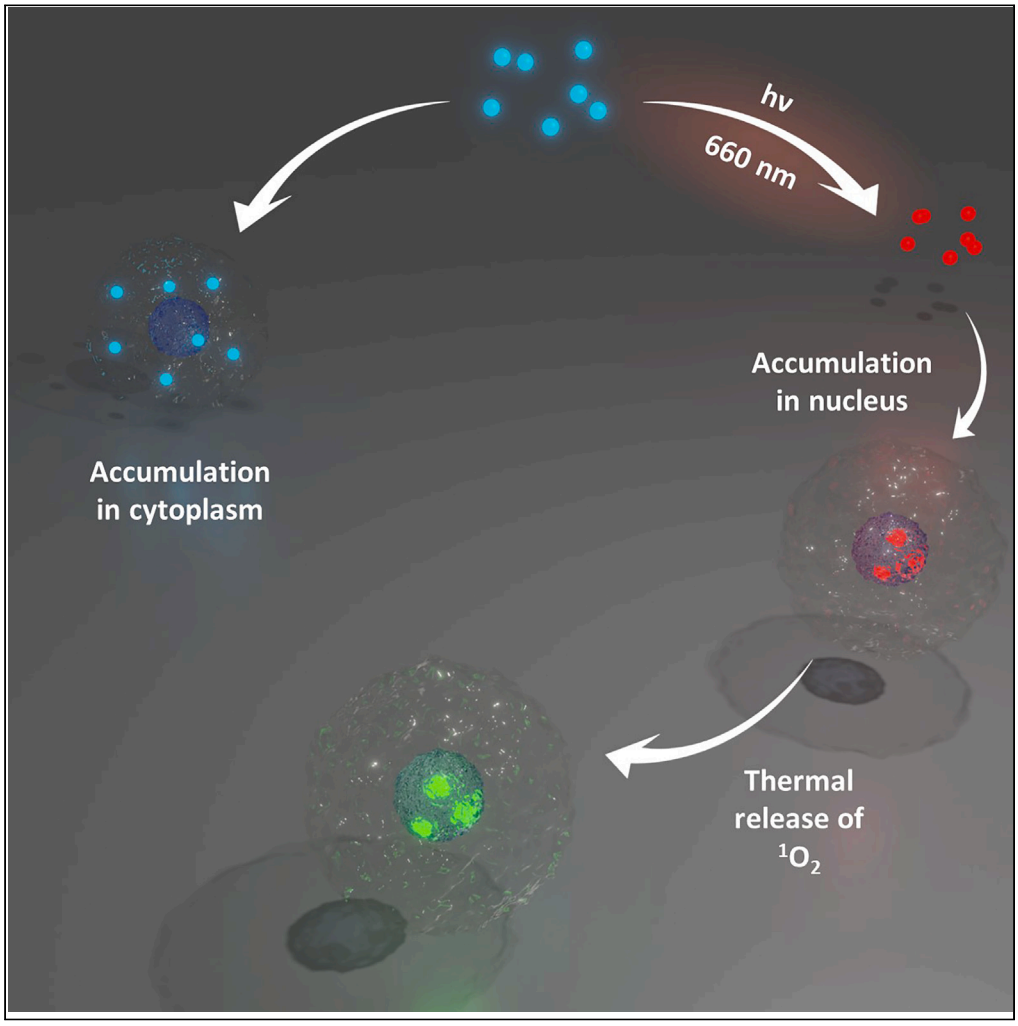

Zakaria Ziani, Saioa Cobo, Nathalie Berthet, Guy Royal

nathalie.berthet@univ-grenoble-alpes.fr (N.B.)
guy.royal@univ-grenoble-alpes.fr (G.R.)

Highlights

A bis-platinum complex incorporating a photochromic unit was investigated

Red-light illumination of the complex under air generates an endoperoxide form

Interaction with DNA and penetration efficiency in cells is photo-modulated

The photogenerated system is able to transport and release $^1O_2$ inside the nucleus

Ziani et al., iScience 27, 108704
January 19, 2024
https://doi.org/10.1016/j.isci.2023.108704

iScience

CellPress
OPEN ACCESS

Article

Optical modulation of cell nucleus penetration and singlet oxygen release of a switchable platinum complex

Zakaria Ziani,[1] Saioa Cobo,[1] Nathalie Berthet,[1,*] and Guy Royal[1,2,*]

SUMMARY

The activation of anticancer molecules with visible light constitutes an elegant strategy to target tumors and to improve the selectivity of treatments. In this context, we report here a visible-light activatable bis-platinum complex (DHP-Pt_2) incorporating an organic photo-switchable ligand based on the dimethyldihydropyrene moiety. Illumination of this metal complex with red light (660 nm) under air readily produces the corresponding endoperoxide form ($CPDO_2$-Pt_2). These two metal complexes exhibit different DNA binding properties and, more importantly, we show that only the photogenerated $CPDO_2$-Pt_2 is able to penetrate into cancer cell nuclei, where it is then capable of releasing cytotoxic singlet oxygen. This study represents the first proof-of-concept showing that dimethyldihydropyrene derivatives can be used to transport and deliver singlet oxygen into cancer cell nuclei upon visible-light activation.

INTRODUCTION

Nowadays, several efficient chemotherapies and therapeutic agents are available.[1–3] However, traditional anti-cancer drugs such as cisplatin and its derivatives suffer from a lack of selectivity that generates many important side effects.[4–8] In this context, the use of photopharmacology[9–12] and photoactivated chemotherapy (PACT)[13–15] constitutes efficient solutions to target cancerous cells and to reach a better specificity since the photochemical activation of the drugs allows a precise spatial and temporal activation of the system.[13,14]

In particular, light-responsive molecular systems and therapies have been developed using coordination complexes. In these systems, the photoactivation is usually metal-centered and the formation of the excited state is followed by a variety of effects and mechanisms that allow the therapeutic effects.[16–18] In 2015, Pérez-Tomás and Gamez proposed an innovative approach in which the PACT technique relies on the optical activation of a coordinated switchable ligand.[19] In their systems, the properties of the metal complexes have been modulated through the isomerization of an organic dithienylethene unit which have been triggered by light irradiation at precise wavelengths. These photochromic complexes were shown to exhibit two photo-interconvertible isomers that display distinct DNA-interacting properties and cytotoxic behaviors against cancer cell lines.[19,20]

The major drawback of photochromic systems to extend their use to biological and medical applications is that their excited state is usually reached by UV light irradiation. Indeed, such light source must be avoided because of its short penetration length into the tissue and because it also causes severe damages.[12,21–23] A strategy to solve this problem is to use a negative photochrom, i.e., a system in which the initial and thermodynamically stable state corresponds to the colored one that can thus be activated by visible light.[24]

In this context, we report herein the study of a bimetallic-platinum(II) complex (**DHP-Pt_2**, Figure 1) in which the two metal centers are bridged through a photoactive bis-pyridine-dimethyldihydropyrene ligand. The dimethyldihydropyrene (**DHP**, closed isomer) unit is an organic and negative photochrom that can be excited with visible light to yield the corresponding cyclophanediene (**CPD**, open form) isomer following the opening of its central carbon-carbon bond.[25–31] In addition to this photochromic behavior that can be exploited for many domains,[21,32–39] we previously reported that some **DHP** derivatives, upon suitable chemical functionalization, may readily lead to an endoperoxide-cyclophanediene (**$CPDO_2$**) form when irradiated with visible (red) light under aerobic conditions.[40–43] In this reaction, the **DHP** form is isomerized into its corresponding cyclophanediene isomer (**CPD**) and, in parallel, it can also act as a photosensitizer and produce singlet oxygen ($^1O_2$) when illuminated under air. The photogenerated **CPD** isomer and $^1O_2$ then react together to yield the corresponding endoperoxide (**$CPDO_2$**). Finally, this compound is able to thermally release a cytotoxic singlet oxygen molecule (typically at 37°C).[40,41] These photoactivable systems are thus able to store, transport and deliver singlet oxygen whose toxicity can be explored in particular for life sciences.

Based on these peculiar properties of DHP derivatives, we report herein the preparation and characterization of the bis-platinum(II) **DHP-Pt_2** complex as well as its corresponding endoperoxide form **$CPDO_2$-Pt_2** (Figure 1) and we investigate the DNA-binding properties and cytotoxic features of these two forms in cancer cells.

[1]University Grenoble Alpes, CNRS, DCM, 38000 Grenoble, France
[2]Lead contact
*Correspondence: nathalie.berthet@univ-grenoble-alpes.fr (N.B.), guy.royal@univ-grenoble-alpes.fr (G.R.)
https://doi.org/10.1016/j.isci.2023.108704

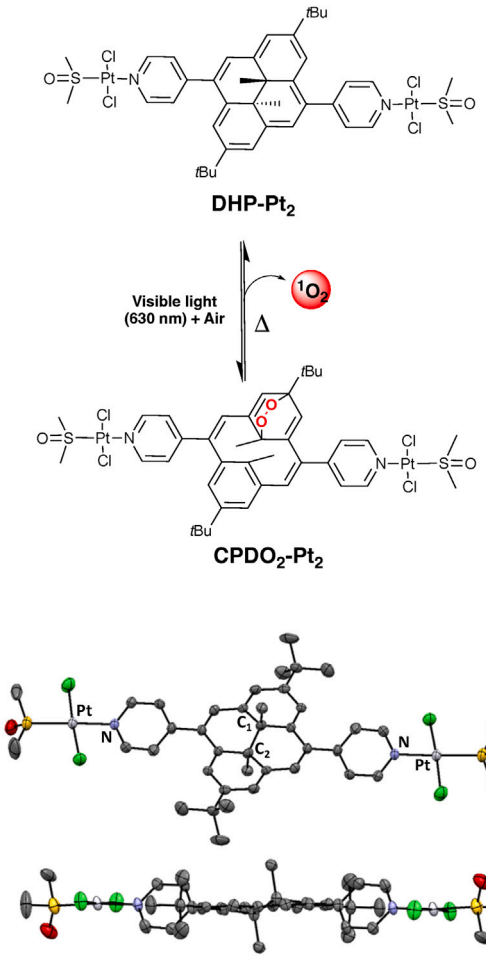

Figure 1. The DHP-Pt_2/$CPDO_2$-Pt_2 system

Top: reversible conversion of the **DHP-Pt_2**/**$CPDO_2$-Pt_2** couple. Down: molecular structure of **DHP-Pt_2** (ORTEP view). Thermal ellipsoids are scaled to a 50% probability level. Hydrogen atoms have been omitted for clarity.

RESULTS AND DISCUSSION

Preparation and characterization of DHP-Pt_2 and $CPDO_2$-Pt_2

The starting bis-pyridine-**DHP** ligand (2,7-di-*tert*-butyl-4,9-di-(4-pyridyl)-*trans*-10b,10c-dimethyl-10b,10c-dihydropyrene; **DHP-Py_2**) was synthesized following our previously reported procedure, using a Suzuki coupling reaction (See supplemental information).[40,44] The **DHP-Pt_2** complex was then prepared by dissolving 2 equivalents of (*cis*-$[Pt(DMSO)_2Cl_2]$[45] in MeOH, followed by the addition of 1 M equivalent of the organic **DHP-Py_2** ligand. Upon stirring, at room temperature (RT) during 12 h under dark conditions, a precipitate was formed and **DHP-Pt_2** was isolated as a brown powder upon filtration. Mass spectrometry as well as ^1H and ^{13}C NMR spectroscopy analysis were in full accordance with the proposed bimetallic structure. In particular, in addition to the signals of the aromatic part of the **DHP** core and of the pyridine groups, ^1H-NMR data (see Figure 2A) show the presence of a unique singlet at $\delta = -3.72$ ppm (6H) corresponding to the signature of the two internal methyl groups of the symmetrical photochromic unit in its closed form. Crystals of **DHP-Pt_2** were further obtained by slow diffusion of Et_2O in a CH_3CN solution and the structure of the complex was confirmed by single-crystal X-ray diffraction (Figure 1).[46] **DHP-Pt_2** crystallizes in a monoclinic system. In this structure, the two metal centers exist in a slightly distorted square planar geometry, their coordination sites being ensured by one pyridine unit, one dimethyl sulfoxide (DMSO) molecule and 2 chloride units in *trans* positions. The distance between the two internal sp^3 carbon (C_1-C_2) is 1.50 Å, which is in accordance with other DHP derivatives.[40,44] In addition, in the solid state, the pyridine units adopt a coplanar arrangement, with dihedral angles of 57° with respect to the main DHP plane.

The absorption spectrum of a CH_2Cl_2 solution of **DHP-Pt_2** (Figure 2C) displays several bands in the visible range attributed to $\pi \rightarrow \pi^*$ transitions that implies singlet electronic excited states of the chromophore core.[25] In particular, the lowest energy transition $S_0 \rightarrow S_1$ is located at 668 nm in **DHP-Pt_2**.

The reactivity of **DHP-Pt_2** toward light was then tested. First, the photosensitizing properties were verified by measuring the production of singlet oxygen during illumination of the compound with red light and under aerobic conditions (air, p = 1 atm, 20°C). For this, the emission band of $^1O_2$ at 1270 nm was measured (see supplemental information) and the results showed that $^1O_2$ was readily produced with a quantum yield of $\varphi_\Delta = 38 \pm 3\%$.

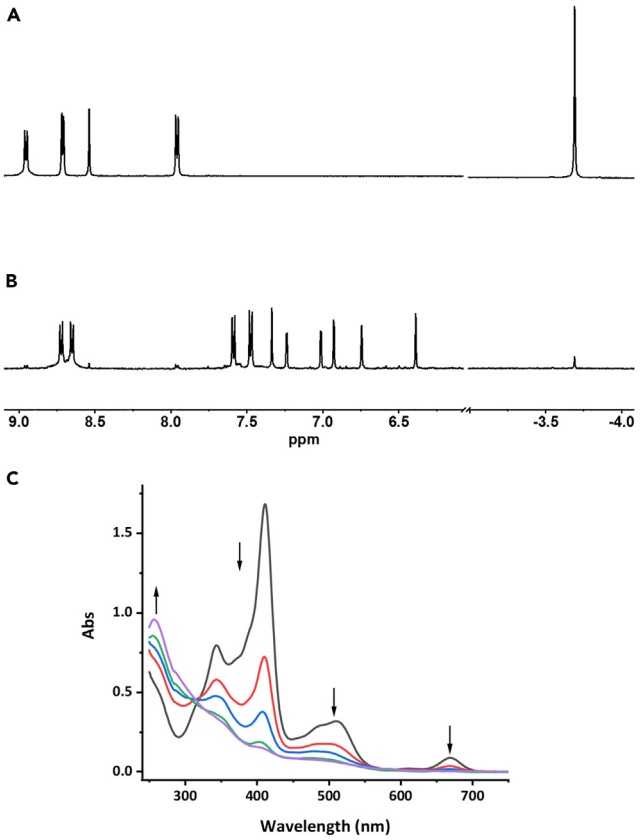

Figure 2. NMR and UV-vis spectroscopic characterization

Partial NMR spectra of a solution of **DHP-Pt$_2$** (~2 mg in 600 µL in CD_2Cl_2) before (A) and after (B) 1 h irradiation with visible light.

(C) UV/Vis spectra evolution of a solution of **DHP-Pt$_2$** in CH_2Cl_2 under air during irradiation with red light (corresponding to the formation of **CPDO$_2$-Pt$_2$**; total time: 20 min). Irradiation conditions: $\lambda > 630$ nm, T = 20°C.

The preparation of the corresponding cyclophanediene-endoperoxide form (**CPDO$_2$-Pt$_2$**, Figure 1) could be then realized by illumination of **DHP-Pt$_2$** in CH_2Cl_2 with red light (λ_{exc} = 660 nm) at RT and under aerobic conditions (air, p = 1 atm). This reaction was followed by UV/Vis spectroscopy (Figure 2C). In accordance with the photo-opening of the central carbon-carbon bond, a discoloration of the solution was observed (from orange to light yellow). This was accompanied by the progressive disappearance of the visible bands of the absorption spectrum and the growth of a new signal in the UV part.

The formation of **CPDO$_2$-Pt$_2$** was confirmed by ^{1}H NMR spectroscopy (Figure 2B). Upon irradiation under air of the **DHP-Pt$_2$** isomer in CD_2Cl_2, a new set of peaks were obtained and their analysis indicated a loss in symmetry, in accordance with the formation of the endoperoxide form. In particular, the signal of the internal methyl groups in the **DHP** state (singlet at $\delta \approx -3.7$ ppm, 6H) disappeared and two new singlets (2 × 3H) were observed at $\delta \sim +1.5$ ppm and 0 ppm, this latter being typical of the signal of the internal methyl group connected to the peroxide function in **CPD-O$_2$** derivatives.[41] In addition, mass spectrometry analysis corroborated the presence of two additional oxygen atoms in the compound upon illumination (See Figures S10 and S11). Finally, **CPDO$_2$-Pt$_2$** was isolated by evaporation of the solvent under vacuum at low temperature (4°C).

At this stage, it is important to outline that the particular (photo)reactivity of dimethyldihydropyrenes toward dioxygen requires a chemical functionalization by suitable electron-withdrawing groups that modify their underlying photochemical mechanisms.[33,43,44] In particular, unlike the **DHP-Pt$_2$** metal complex, the bis-pyridine **DHP-Py$_2$** ligand does not form endoperoxides and cannot be isomerized by red light irradiation. Therefore, the presence of the platinum centers is clearly essential in this work.

The reversion process between **CPDO$_2$-Pt$_2$** and **DHP-Pt$_2$** forms and consequent release of $^1O_2$ were thermally evaluated at 25°C using NMR studies. After 48 h, the endoperoxide form totally disappeared and a major part of **DHP-Pt$_2$** was recovered. It should be noted that some undefined products were also formed, certainly due to some oxidation reactions occurring during the experiment.

The fluorescence properties of **DHP-Pt$_2$** and **CPDO$_2$-Pt$_2$** have been also examined. Whereas **CPDO$_2$-Pt$_2$** does not exhibit any emission, the **DHP-Pt$_2$** complex displays a narrow fluorescence signal at 687 nm upon excitation at 450 nm (Figure S1). The relatively small value of the Stokes Shift (−0.0514 eV) indicates that the geometry in the first excited state (S_1) and in the ground state (S_0) of **DHP-Pt$_2$** are close. The radiative deexcitation from the first excited state was found to be mono-exponential with an associated lifetime τ = 2.2 ns and a fluorescence

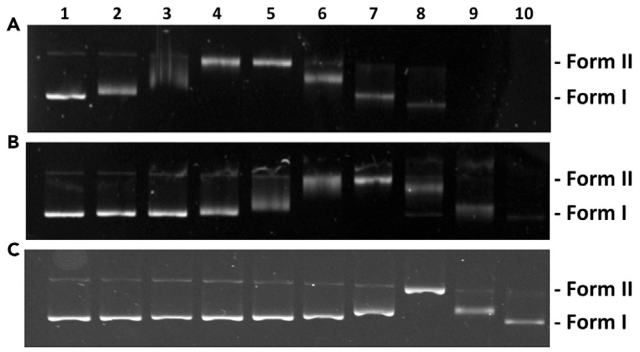

Figure 3. Interaction of DHP-Pt_2 and $CPDO_2$-Pt_2 with DNA

Agarose gel electrophoresis images of pBR322 DNA plasmid (13 μg mL^{-1}) incubated for 16 h at 37°C with increasing concentrations of (A) **DHP-Pt_2**, (B) **$CPDO_2$-Pt_2** and (C) cisplatin. Lane 1: pure plasmid DNA; lanes 2–10: 0.09, 0.19, 0.39, 0.78, 1.56, 3.12, 6.25, 12.5, 25 μM of compound.

quantum yield of $\varphi_f = 8.6.10^{-3}$. These differences in the fluorescence properties between **DHP-Pt_2** and **$CPDO_2$-Pt_2** can be utilized to identify the state of the system, in particular in biological media.

Biological investigations

Following the previous experiments, the biological properties of **DHP-Pt_2** and **$CPDO_2$-Pt_2** were investigated. The interaction of the two metallic complexes with DNA was first studied by measuring the electrophoretic mobility in an agarose gel of pBR322 DNA plasmid treated with increasing concentrations of each compound. DNA treated with cisplatin (*cis*-diamminedichloroplatinum(II)) was also used for comparison. Figure 3 shows the electrophoretic migration patterns of DNA plasmid for each condition.

Before any treatment, DNA plasmid was essentially composed of supercoiled form I and some small fraction of relaxed circular form II. When incubated with increasing concentrations of platinum compounds, a proportional decrease in the electrophoretic mobility of the supercoiled DNA plasmid form I and increase in that of the relaxed circular form II were observed until both forms comigrates. The lower mobility of the DNA form I is a consequence of DNA unwinding and removal of negative supercoils due to the interaction of the metallocomplexes. When the concentration was further increased, a positively supercoiled DNA migrated faster into the agarose gel. The concentration for which the two bands (DNA forms I and II) are coalescent is currently used as an indicator of the DNA unwinding relative to the effectiveness of compounds to interact with DNA and to form adducts with nucleobases.[47–49] It has to be mentioned that no change in the electrophoretic mobility of the DNA (forms I and II) has been detected when plasmid was incubated with the bis-pyridine-**DHP** ligand (Figure S3).The point of coalescence for DNA treated with cisplatin was obtained at a concentration of 6.25 μM (Figure 3C, lane 8) while it was observed at 16 and 4 times lower concentrations for DNA treated with **DHP-Pt_2** and **$CPDO_2$-Pt_2** respectively (Figure 3A, lane 4; Figure 3B, lane 6), suggesting a better interaction of the bis-platinum compounds with DNA compared to cisplatin. More importantly, comigration of DNA forms I and II was observed at a **DHP-Pt_2** concentration 4 times lower than **$CPDO_2$-Pt_2** (0.39 μM and 1.56 μM respectively) indicating that these two compounds interact differently with DNA. This result may be attributed to the difference in geometry between the starting DHP complex and the photogenerated endoperoxide form. Indeed, the flat aromatic part of **DHP-Pt_2** (Figure 1) may facilitate its interaction with DNA and thus promotes the formation of covalent bonds with nucleobases. In contrast, **$CPDO_2$-Pt_2** is expected to exhibit a very different shape due to the photo-opening of the central C-C bond followed by the formation of the C-O-O-C bridge that leads to a change in the hybridization states of the carbon atoms, from sp^2 to sp^3 and this structure is certainly less conducive to interaction with DNA.[41]

Cell viability was next investigated with four cancer cell lines, BT-549 (human breast ductal carcinoma), HeLa (human cervical carcinoma), A-549 (human lung adenocarcinoma) and A-375 (human melanoma). In a first assay, all cancer cell lines were incubated for 48 h with a single concentration of 50 μM of **DHP-Pt_2** or **$CPDO_2$-Pt_2** and their viabilities were measured using standard MTT assays. Results are depicted in Figure 4. A disparity in cell viability among the various lines treated with the bis-platinum complexes was clearly noticed. The lowest cell viabilities were measured with A-375 (**DHP-Pt_2**: 50.42%, **CPDO2-Pt_2** 56.80%) and HeLa (**DHP-Pt_2**: 57.15% and **$CPDO_2$-Pt_2**: 63.69%), while very modest or even no effect on the cell viability was observed with A-549 and BT-549 (A-549 cell viability: 80.99% with **DHP-Pt_2** and 76.94% with **$CPDO_2$-Pt_2**). For all cell lines, no significant difference in cell viability at 48 h was measured based on whether they were treated with 50 μM of **DHP-Pt_2** or **$CPDO_2$-Pt_2**.

IC_{50} values at 24, 48 and 72 h of incubation with **DHP-Pt_2**, **$CPDO_2$-Pt_2** and cisplatin were then determined for cells that showed a greater sensitivity toward the bis-platinum compounds in the first viability assay (A-375 and HeLa; results are reported in Table S2). Compounds cytotoxicity was also investigated at 48h with HFF-1 non-cancer cells (human foreskin fibroblasts).The data were consistent with those obtained with the first single point toxicity assay, showing very similar cytotoxicity properties for both **DHP-Pt_2** and **$CPDO_2$-Pt_2** after 24, 48 or 72 h of incubation with both cancer cell lines (IC_{50} values at 48 h, for **DHP-Pt_2**/**$CPDO_2$-Pt_2** 52.5 μM versus 56.2 μM with A-375 and 59.8 μM versus 61.9 μM with HeLa). It should be pointed out that these IC_{50} values remain higher than those determined with cisplatin, certainly because of the lower ability of the compounds to cross the cell membrane and penetrate the nucleus compared to the small cisplatin molecule. However, an important point to mention is that **DHP-Pt_2** and **$CPDO_2$-Pt_2** were found to be more toxic on both cancer cell lines than on healthy HFF-1 cells (see Table S2).

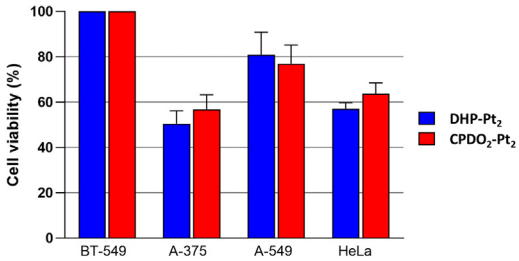

Figure 4. Cancer cell viability studies in the presence of DHP-Pt_2 and $CPDO_2$-Pt_2

Cell-viability assay with **DHP-Pt_2** or **$CPDO_2$-Pt_2** performed with four human cancer cell lines, BT-549 (breast carcinoma), HeLa (cervical carcinoma), A-549 (lung adenocarcinoma) and A-375 (melanoma). Assays were conducted using a concentration in each bis-platinum complex of 50 μM and an incubation time of 48 h. Percentages in cell viability are reported.

It is important to note that the close cytotoxic properties measured for both compounds contrast with the lower ability for **$CPDO_2$-Pt_2** to interact with DNA compared to **DHP-Pt_2.** This result suggests that different cytotoxic processes may be involved for cells treated with these two complexes. To corroborate this hypothesis, the potential of each of the two bis-platinum complexes to penetrate cells and reach the nucleus was examined. For this, the presence of **DHP-Pt_2** was measured by confocal microscopy using its fluorescence properties. The cellular uptake of both bis-platinum compounds with A-375 cell line (for which the higher cytotoxicity was observed) and with BT-549 (that exhibits a low sensitivity toward the compounds) was detected. Analyze of cell fluorescence indicated that the penetration of **DHP-Pt_2** and **$CPDO_2$-Pt_2** into cell lines is clearly different (Figure 5).

Indeed, while most of the **DHP-Pt_2** molecules appeared accumulated into the cell cytoplasm of A-375 cells, important amounts of **$CPDO_2$-Pt_2** were capable to enter into the nucleus (and were then detected as their **DHP-Pt_2** form upon their singlet O_2 release; *vide infra*). For BT-549 cells, used as negative control, both compounds penetrated the cell membrane but did not reach the nucleus. These observations could explain the low cytotoxicity of the compounds with this cell line. To confirm these observations, the fluorescence intensity profiles of the bis-platinum compounds and the nuclear marker (Hoechst 33342), in both cancer cell lines have been analyzed (see Figure S4). As clearly shown by the colocalization profiles, only **$CPDO_2$-Pt_2** enters the A-375 cell nucleus demonstrating that the penetration of the bis-platinum complex in the nuclear compartment depends on the (photo)state of the system.

As written previously, a great asset of endoperoxide derivatives, photogenerated from DHP systems, deals with their ability to thermally release singlet oxygen.[40,41] The reactive oxygen species (ROS) cell delivery with this platinum complex was thus investigated by microscopy. For this, 2′,7′-dichlorodihydrofluorescein diacetate (DCFH-DA) was used as an ROS probe to evidence the intracellular delivery of $^1O_2$.[50] A-375 cells pre-treated with DCFH-DA were incubated with 10 μM of **$CPDO_2$-Pt_2** or **DHP-Pt_2** (that was used as a negative control since it was not expected to release singlet oxygen) and the cell fluorescence was examined by confocal microscopy (Figure 6). Whereas significant cell fluorescence was observed for cells treated with **$CPDO_2$-Pt_2**, no emission was detected with **DHP-Pt_2**. This important result shows that it is possible to control the transportation and release of cytotoxic $^1O_2$ in cell nuclei using the endoperoxide form of the platinum complex.

Limitations of the study

This study shows that **DHP-Pt_2** and **$CPDO_2$-Pt_2** exhibit different mechanisms of cytotoxicity. Indeed, **DHP-Pt_2** has higher interactions with DNA while only **$CPDO_2$-Pt_2** is able to enter in the nuclear compartment and to release toxic singlet dioxygen. However, the difference in the cytotoxicity of the two states, i.e., before and after illumination, must be improved in order to avoid side effects. This can be done by

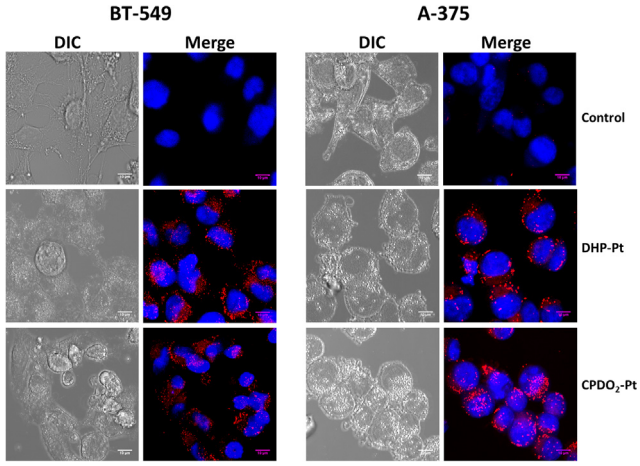

Figure 5. Penetration studies of DHP-Pt_2 and $CPDO_2$-Pt_2 into cell lines

Confocal fluorescence microscopic images of BT-549 and A-375 cells treated with 25 μM of **DHP-Pt_2** or **$CPDO_2$-Pt_2** for 24 h at 37°C. The merged images were obtained from Z-stacks of one of the platinum complexes (red) and nuclear marker Hoechst (blue).

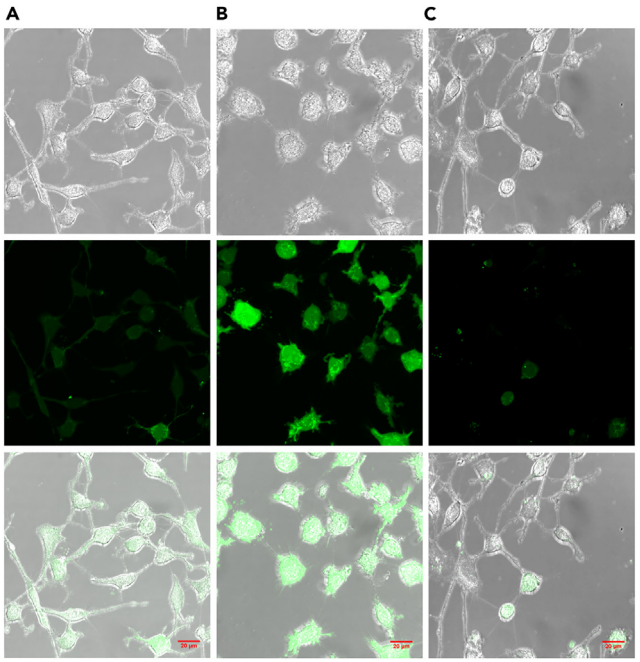

Figure 6. Singlet oxygen release in tumor cells

Imaging of the $^1O_2$ release from complexes inside cultured A-375 cells using DCFH-DA as intracellular ROS probe. (A) incubation with 10 μM **DHP-Pt$_2$**, (B) incubation with 10 μM **CPDO$_2$-Pt$_2$**, (C) control cells without platinum complex. Top row DIC, middle row fluorescence image, bottom, merged. Scale bar is 20 μm.

further chemical modification of the platinum complex. In addition, the selectivity of the system can be increased by introducing appropriate vectors targeting proteins overexpressed in tumor tissues, enabling accumulation of the platinum complex specifically in cancer cells.

Conclusion

In summary, we have synthetized and investigated a new photoswitchable bis-platinum complex, **DHP-Pt$_2$**, based on the organic dimethyldihydropyrene core. **DHP-Pt$_2$** can be readily converted upon red-light illumination under aerobic conditions into its corresponding endoperoxide form **CPDO$_2$-Pt$_2$**. The biologic evaluation of **DHP-Pt$_2$** and **CPDO$_2$-Pt$_2$** revealed their different abilities to interact with DNA. In contrast, these two platinum complexes exhibited similar cytotoxic properties against A-375 cells line, suggesting that the lower ability of **CPDO$_2$-Pt$_2$** to interact with DNA and form toxic adducts with nucleobases, is compensated by a different mechanism of cytotoxicity and in particular by the release of $^1O_2$. This hypothesis was supported by further experiments that demonstrate a high penetration of the bis-platinum complex in the nuclear compartment only under its endoperoxide state. In addition, the **CPDO$_2$-Pt$_2$** form is capable to thermally release toxic singlet dioxygen inside the nucleus. Several therapeutic effects (due to the platinum centers and to the production of singlet O_2) can be thus photo-triggered and accumulated in the same molecular system.

This work represents the first example of biological investigations of dimethyldihydropyrenes capable of singlet oxygen production. We believe that these results open new perspectives in the domain of photopharmacology, especially for therapeutics targeting hypoxic tumor cells and hypoxic microenvironments. Our next steps will be to improve the therapeutic effects by further chemical functionalization of the system and to investigate *in vitro* and *in vivo* studies with *in situ* illuminations.

STAR★METHODS

Detailed methods are provided in the online version of this paper and include the following:

- KEY RESOURCES TABLE
- RESOURCE AVAILABILITY
  - Lead contact
  - Materials availability
  - Data and code availability
- METHOD DETAILS
  - Synthesis
  - Preparation of DHP-Pt$_2$
  - Preparation of CPDO$_2$-Pt$_2$

- X-Ray diffraction
- Spectroscopy
- Irradiation procedures
- Singlet oxygen production (Φ_Δ)
- Confocal microscopy
- Cell lines and culture conditions
- Interaction with DNA plasmid
- Intracellular singlet oxygen release
- Cell viability assay
- Confocal microscopy for cell-compound localization

SUPPLEMENTAL INFORMATION

Supplemental information can be found online at https://doi.org/10.1016/j.isci.2023.108704.

ACKNOWLEDGMENTS

This work was supported by the Labex ARCANE (ANR-11-LABX-003) and the French Agence National de la Recherche (ANR-18-CE29-0012 PHOTOCHROMICS). The NanoBio ICMG (UAR2607) is acknowledged for providing facilities for mass spectrometry analyses (Amélie Durand, Laure Fort, Rodolphe Gueret) as well as the DCM (Département de Chimie Moléculaire, Plateau Technique de Synthèse) for the synthesis of the DHP precursors (Martine Fayolle, Mathieu Curtil, Pierre-Yves Chavant). We thank Cécile Cottet (LBFA, Grenoble) for confocal microscopy experiments and for giving access to flow cytometer. Clara Hermant, Samuel Decorps and Rémy Lartia (DCM Grenoble) are also warmly acknowledged for their help.

AUTHOR CONTRIBUTIONS

G.R. and N.B. were in charge of the project administration, conceived and supervised the project. Z.Z. carried out the main characterizations and collected the data. S.C. synthetized the platinum complex and did its NMR and mass spectrometry analysis. G.R. was in charge of the (photo)chemical part and N.B. of the biological investigations. All authors discussed and analyzed the results, and contributed to the editing of the manuscript. N.B. and G.R. acquired funding.

DECLARATION OF INTERESTS

The authors declare no competing interests.

Received: June 28, 2023
Revised: October 6, 2023
Accepted: December 7, 2023
Published: December 9, 2023

REFERENCES

1. R.T. Skeel, and S.N. Khleif, eds. (2011). Handbook of cancer chemotherapy, Eighth Edition (Wolter Kluwer).
2. Zhong, L., Li, Y., Xiong, L., Wang, W., Wu, M., Yuan, T., Yang, W., Tian, C., Miao, Z., Wang, T., and Yang, S. (2021). Small molecules in targeted cancer therapy: advances, challenges, and future perspectives. Signal Transduct. Targeted Ther. *6*, 201.
3. American Chemical Society, American Chemical Society, and American Chemical Society (2001). Anticancer Agents: Frontiers in Cancer Chemotherapy, I. Ojima, G.D. Vite, and K.-H. Altmann, eds. (American Chemical Society).
4. Lippard, S.J. (1982). New Chemistry of an Old Molecule: cis-[$Pt(NH_3)_2Cl_2$]. Science *218*, 1075–1082.
5. Lowenthal, R.M., and Eaton, K. (1996). Toxicity of chemotherapy. Hematol. Oncol. Clin. N. Am. *10*, 967–990.
6. Rabik, C.A., and Dolan, M.E. (2007). Molecular mechanisms of resistance and toxicity associated with platinating agents. Cancer Treat Rev. *33*, 9–23.
7. Oun, R., Moussa, Y.E., and Wheate, N.J. (2018). The side effects of platinum-based chemotherapy drugs: a review for chemists. Dalton Trans. *47*, 6645–6653.
8. A. Bonetti, R. Leone, F.M. Muggia, and S.B. Howell, eds. (2009). Platinum and Other Heavy Metal Compounds in Cancer Chemotherapy: Molecular Mechanisms and Clinical Applications (Humana Press).
9. Lerch, M.M., Hansen, M.J., van Dam, G.M., Szymanski, W., and Feringa, B.L. (2016). Emerging Targets in Photopharmacology. Angew. Chem. Int. Ed. *55*, 10978–10999.
10. Velema, W.A., Szymanski, W., and Feringa, B.L. (2014). Photopharmacology: Beyond Proof of Principle. J. Am. Chem. Soc. *136*, 2178–2191.
11. Szymański, W., Beierle, J.M., Kistemaker, H.A.V., Velema, W.A., and Feringa, B.L. (2013). Reversible Photocontrol of Biological Systems by the Incorporation of Molecular Photoswitches. Chem. Rev. *113*, 6114–6178.
12. Volarić, J., Szymanski, W., Simeth, N.A., and Feringa, B.L. (2021). Molecular photoswitches in aqueous environments. Chem. Soc. Rev. *50*, 12377–12449.
13. Shi, H., and Sadler, P.J. (2020). How promising is phototherapy for cancer? Br. J. Cancer *123*, 871–873.
14. Bonnet, S. (2018). Why develop photoactivated chemotherapy? Dalton Trans. *47*, 10330–10343.
15. Farrer, N.J., Salassa, L., and Sadler, P.J. (2009). Photoactivated chemotherapy (PACT): the potential of excited-state d-block metals in medicine. Dalton Trans. 10690–10701.
16. Van Geest, E.P., Götzfried, S.K., Klein, D.M., Salitra, N., Popal, S., Husiev, Y., Van Der Griend, C.J., Zhou, X., Siegler, M.A., Schneider, G.F., and Bonnet, S. (2023). A Lock-and-Kill Anticancer Photoactivated Chemotherapy Agent. Photochem. Photobiol. *99*, 777–786.
17. Chen, Y., Bai, L., Zhang, P., Zhao, H., and Zhou, Q. (2021). The Development of Ru(II)-Based Photoactivated Chemotherapy Agents. Molecules *26*, 5679.
18. Panwar, A., Pal, M., and Roy, M. (2023). Photochemical aspects of iron complexes

exhibiting photo-activated chemotherapy (PACT). J. Inorg. Biochem. *238*, 112055.
19. Presa, A., Brissos, R.F., Caballero, A.B., Borilovic, I., Korrodi-Gregório, L., Pérez-Tomás, R., Roubeau, O., and Gamez, P. (2015). Photoswitching the Cytotoxic Properties of Platinum(II) Compounds. Angew. Chem. Int. Ed. Engl. *54*, 4561–4565.
20. Presa, A., Vázquez, G., Barrios, L.A., Roubeau, O., Korrodi-Gregório, L., Pérez-Tomás, R., and Gamez, P. (2018). Photoactivation of the Cytotoxic Properties of Platinum(II) Complexes through Ligand Photoswitching. Inorg. Chem. *57*, 4009–4022.
21. Klaue, K., Garmshausen, Y., and Hecht, S. (2018). Taking Photochromism beyond Visible: Direct One-Photon NIR Photoswitches Operating in the Biological Window. Angew. Chem. Int. Ed. *57*, 1414–1417.
22. Bléger, D., and Hecht, S. (2015). Visible-Light-Activated Molecular Switches. Angew. Chem. Int. Ed. *54*, 11338–11349.
23. B.L. Feringa, and W.R. Browne, eds (2011). Molecular Switches. Second, Completely Revised and Enlarged Edition, *2* (Wiley-VCH Verlag GmbH & Co. KGaA).
24. Aiken, S., Edgar, R.J., Gabbutt, C.D., Heron, B.M., and Hobson, P.A. (2018). Negatively photochromic organic compounds: Exploring the dark side. Dyes Pigments *149*, 92–121.
25. Sarkar, R., Heitz, M.-C., Royal, G., and Boggio-Pasqua, M. (2020). Electronic Excited States and UV–Vis Absorption Spectra of the Dihydropyrene/Cyclophanediene Photochromic Couple: a Theoretical Investigation. J. Phys. Chem. A *124*, 1567–1579.
26. Boggio-Pasqua, M., and Garavelli, M. (2015). Rationalization and Design of Enhanced Photoinduced Cycloreversion in Photochromic Dimethyldihydropyrenes by Theoretical Calculations. J. Phys. Chem. A *119*, 6024–6032.
27. Ayub, K., Li, R., Bohne, C., Williams, R.V., and Mitchell, R.H. (2011). Calculation Driven Synthesis of an Excellent Dihydropyrene Negative Photochrome and its Photochemical Properties. J. Am. Chem. Soc. *133*, 4040–4045.
28. Bohne, C., and Mitchell, R.H. (2011). Characterization of the photochromism of dihydropyrenes with photophysical techniques. J. Photochem. Photobiol. C Photochem. Rev. *12*, 126–137.
29. Blattmann, H.-R., Meuche, D., Heilbronner, E., Molyneux, R.J., and Boekelheide, V. (1965). Photoisomerization of trans-15,16-Dimethyldihydropyrene. J. Am. Chem. Soc. *87*, 130–131.
30. Blattmann, H.R., and Schmidt, W. (1970). Über die phototropie des trans-15,16-dimethyldihydropyrens und seiner derivate. Tetrahedron *26*, 5885–5899.
31. Mitchell, R.H. (1999). The Metacyclophanediene-Dihydropyrene Photochromic π Switch. Eur. J. Org. Chem. *1999*, 2695–2703.
32. Roldan, D., Kaliginedi, V., Cobo, S., Kolivoska, V., Bucher, C., Hong, W., Royal, G., and Wandlowski, T. (2013). Charge transport in photoswitchable dimethyldihydropyrene-type single-molecule junctions. J. Am. Chem. Soc. *135*, 5974–5977.
33. Ziani, Z., Cobo, S., Loiseau, F., Jouvenot, D., Lognon, E., Boggio-Pasqua, M., and Royal, G. (2023). All Visible Light Photoswitch Based on the Dimethyldihydropyrene Unit Operating in Aqueous Solutions with High Quantum Yields. JACS Au *3*, 131–142.
34. Bakkar, A., Lafolet, F., Roldan, D., Puyoo, E., Jouvenot, D., Royal, G., Saint-Aman, E., and Cobo, S. (2018). Bidirectional light-induced conductance switching in molecular wires containing a dimethyldihydropyrene unit. Nanoscale *10*, 5436–5441.
35. Straight, S.D., Andréasson, J., Kodis, G., Bandyopadhyay, S., Mitchell, R.H., Moore, T.A., Moore, A.L., and Gust, D. (2005). Molecular AND and INHIBIT Gates Based on Control of Porphyrin Fluorescence by Photochromes. J. Am. Chem. Soc. *127*, 9403–9409.
36. Ghosh, S., Hossain, M.S., Chatterjee, S., Rahaman, S.A., and Bandyopadhyay, S. (2020). Light-Gated Modulation of Electronic Mobility of a Dihydropyrene-Based Photochromic Coordination Polymer. ACS Appl. Mater. Interfaces *12*, 52983–52991.
37. Lee, H.-W., Robinson, S.G., Bandyopadhyay, S., Mitchell, R.H., and Sen, D. (2007). Reversible Photo-regulation of a Hammerhead Ribozyme Using a Diffusible Effector. J. Mol. Biol. *371*, 1163–1173.
38. Krishna, V.S.R., Samanta, M., Pal, S., Anurag, N.P., and Bandyopadhyay, S. (2016). Light-triggered assembly–disassembly of an ordered donor–acceptor π-stack using a photoresponsive dimethyldihydropyrene π-switch. Org. Biomol. Chem. *14*, 5744–5750.
39. Fredrich, S., Göstl, R., Herder, M., Grubert, L., and Hecht, S. (2016). Communications Photoswitches Hot Paper Switching Diarylethenes Reliably in Both Directions with Visible Light Angewandte. Angew. Chem. Int. Ed. Engl. *55*, 1208–1212.
40. Ziani, Z., Loiseau, F., Lognon, E., Boggio-Pasqua, M., Philouze, C., Cobo, S., and Royal, G. (2021). Synthesis of a Negative Photochrome with High Switching Quantum Yields and Capable of Singlet-Oxygen Production and Storage. Chem. Eur J. *27*, 16642–16653.
41. Cobo, S., Lafolet, F., Saint-Aman, E., Philouze, C., Bucher, C., Silvi, S., Credi, A., and Royal, G. (2015). Reactivity of a pyridinium-substituted dimethyldihydropyrene switch under aerobic conditions: self-sensitized photo-oxygenation and thermal release of singlet oxygen. Chem. Commun. *51*, 13886–13889.
42. Bakkar, A., Cobo, S., Lafolet, F., Saint-Aman, E., and Royal, G. (2015). A new surface-bound molecular switch based on the photochromic dimethyldihydropyrene with light-driven release of singlet oxygen properties. J. Mater. Chem. C *3*, 12014–12017.
43. Boggio-Pasqua, M., López Vidal, M., and Garavelli, M. (2017). Theoretical mechanistic study of self-sensitized photo-oxygenation and singlet oxygen thermal release in a dimethyldihydropyrene derivative. J. Photochem. Photobiol. Chem. *333*, 156–164.
44. Roldan, D., Cobo, S., Lafolet, F., Vilà, N., Bochot, C., Bucher, C., Saint-Aman, E., Boggio-Pasqua, M., Garavelli, M., and Royal, G. (2015). A Multi-Addressable Switch Based on the Dimethyldihydropyrene Photochrome with Remarkable Proton-Triggered Photo-opening Efficiency. Chem. Eur J. *21*, 455–467.
45. Price, J.H., Williamson, A.N., Schramm, R.F., and Wayland, B.B. (1972). Palladium(II) and platinum(II) alkyl sulfoxide complexes. Examples of sulfur-bonded, mixed sulfur- and oxygen-bonded, and totally oxygen-bonded complexes. Inorg. Chem. *11*, 1280–1284.
46. Deposition Number CCDC-2240890 (For DHP-Pt2) Contains the Supplementary Crystallographic Data for This Paper. These Data Are provided Free of Charge by the Joint Cambridge Crystallographic Data Centre and Fachinformationszentrum Karlsruhe Service
47. Cohen, R.L. (1971). Substituent effects on the reactivity of triarylimidazolyl free radicals toward tris(2-methyl-4-diethylaminophenyl) methane. J. Org. Chem. *36*, 2280–2284.
48. Cohen, G.L., Bauer, W.R., Barton, J.K., and Lippard, S.J. (1979). Binding of cis - and trans -Dichlorodiammineplatinum(II) to DNA: Evidence for Unwinding and Shortening of the Double Helix. Science *203*, 1014–1016.
49. Johnson, B.W., Burgess, M.W., Murray, V., Aldrich-Wright, J.R., and Temple, M.D. (2018). The interactions of novel mononuclear platinum-based complexes with DNA. BMC Cancer *18*, 1284.
50. Satoh, T., Sakai, N., Enokido, Y., Uchiyama, Y., and Hatanaka, H. (1996). Free Radical-Independent Protection by Nerve Growth Factor and Bcl-2 of PC12 Cells from Hydrogen Peroxide-Triggered Apoptosis. J. Biochem. *120*, 540–546.
51. Oliveros, E., Bossmann, S.H., Nonell, S., Martí, C., Heit, G., Tröscher, G., Neuner, A., Martínez, C., and Braun, A.M. (1999). Photochemistry of the singlet oxygen [$O_2(^1\Delta_g)$] sensitizer perinaphthenone (phenalenone) in N,N′-dimethylacetamide and 1,4-dioxane. New J. Chem. *23*, 85–93.
52. Bregnhøj, M., Westberg, M., Jensen, F., and Ogilby, P.R. (2016). Solvent-dependent singlet oxygen lifetimes: temperature effects implicate tunneling and charge-transfer interactions. Phys. Chem. Chem. Phys. *18*, 22946–22961.
53. Schweitzer, C., and Schmidt, R. (2003). Physical Mechanisms of Generation and Deactivation of Singlet Oxygen. Chem. Rev. *103*, 1685–1757.
54. Schmidt, R., Tanielian, C., Dunsbach, R., and Wolff, C. (1994). Phenalenone, a universal reference compound for the determination of quantum yields of singlet oxygen $O_2(^1\Delta_g)$ sensitization. J. Photochem. Photobiol. Chem. *79*, 11–17.
55. Moberly, J.G., Bernards, M.T., and Waynant, K.V. (2018). Key features and updates for Origin 2018. J. Cheminf. *10*, 5.
56. Abràmoff, M.D., Magalhães, P.J., and Ram, S.J. (2004). Image Processing with ImageJ. Biophot. Int. *11*, 36–42.
57. Mosmann, T. (1983). Rapid colorimetric assay for cellular growth and survival: Application to proliferation and cytotoxicity assays. J. Immunol. Methods *65*, 55–63.

STAR★METHODS

KEY RESOURCES TABLE

REAGENT or RESOURCE	SOURCE	IDENTIFIER
Biological samples		
pBR322 DNA	Euromedex	cat#10-0441
Chemicals, peptides, and recombinant proteins		
Acetonitrile	Sigma Aldrich	CAS No.: 75-05-8
Tetrahydrofurane	Sigma Aldrich	CAS No.: 109-99-9
Potassium tetrachloroplatinate(II)	Sigma Aldrich	CAS No.: 10025-99-7
Dimethylsulfoxyde	Sigma Aldrich	CAS No.: 67-68-5
Cisplatin	Sigma Aldrich	cat#1134357 CAS No.: 15663-27-1
Agarose	Euromedex	cat#BI-D0012 CAS No.: 9012-36-6
Boric acid	Euromedex	cat#BI-BB0044 CAS No.: 10043-35-3
Tris base	Euromedex	cat#26-128-3094-B CAS No.: 77-86-1
Urea	Euromedex	cat#EU0014-B CAS No.: 57-13-6
DCFHDA	Sigma Aldrich	cat#35845 CAS No.: 2044-85-1 ID: 57649438
bis Benzimide H 33342 trihydrchloride (Hoeschst 33342)	Sigma Aldrich	cat#B2261 CAS No.: 875756-97-1 ID: 24891639
MTT	Sigma Aldrich	cat#475989 CAS No.: 298-93-1
Dulbecco's modified Eagle"s medium (DMEM)	Sigma Aldrich	cat#D0819
RPMI-1640 Medium	Sigma Aldrich	cat#R2405
Fetal Bovine Serum (FBS)	Sigma Aldrich	cat#F7524
penicillin-Streptomycin	Sigma Aldrich	cat#P4458
Phosphate Buffered Saline (PBS)	Sigma Aldrich	cat#806552
Trypsin-EDTA	Sigma Aldrich	cat#T2610
phenalenone	Sigma Aldrich	cat#P10801 CAS No.: 548-39-0
Experimental models: Cell lines		
BT-549	ATCC	Cat#HTB-122
HeLa	ATCC	Cat#CCL-2
A-549	ATCC	Cat#CCL-185
A-375	ATCC	Cat#CRL-1619
Software and algorithms		
ImageJ software	https://imagej.net/ij	

RESOURCE AVAILABILITY

Lead contact

Lead contact: Guy Royal (guy.royal@univ-grenoble-alpes.fr). Information and requests should be directed to Nathalie Berthet (nathalie.berthet@univ-grenoble-alpes.fr) for biological studies or Guy Royal for (photo)chemical studies.

Materials availability

This study did not generate new materials.

Data and code availability

Crystallographic structure of **DHP-Pt$_2$** can be obtained free of charge from The Cambridge Crystallographic Data Centre via www.ccdc.cam.ac.uk/data_request/cif. CCDC-2240890 contains the supplementary crystallographic data for this paper. All other datasets, including experimental spectra and data are available in the supplemental information and are publicly available as of the date of publication. This study does not report original code.

METHOD DETAILS

Organic and inorganic reagents used in the synthetic procedures were purchased from Aldrich and were used without additional purification. Solvents were used as received except THF that was distilled over sodium/ benzophenone under argon. pBR322 plasmid DNA, agarose, boric acid, tris base and urea were purchased from Euromedex. 2′,7′-dichlorodihydrofluorescein diacetate (DCFH-DA), Hoechst 33342, 3-(4,5-dimethylthiazol-2-yl)-2,5-diphenyltetrazolium bromide (MTT) and cell culture relevant reagents such Dulbecco's modified Eagle's medium (DMEM), Roswell Park Institute (RPMI)-1640 medium, fetal bovine serum (FBS), antibiotics (penicillin, streptomycin), phosphate buffered saline (PBS), trypsin were all purchased from Sigma-Aldrich Chemical Co., St. Louis, MO, USA.

All evaporations were carried out under reduced pressure with a rotatory evaporator, and all organic extract were washed with water and dried over $MgSO_4$. Merck Kieselgel silica gel, 40-63 μm was used for column chromatography. NMR spectra were performed on a Brucker Avanced 500 or 400 MHz spectrometer using deuterated solvents. Chemicals shifts were calibrated to residual solvent peaks. Coupling constant values (*J*) are given in hertz and chemical shifts (d) in ppm. High-resolution mass spectrometry analyses were conducted using the HRMS, Bruker maXis mass spectrometer and were performed in positive Electrospray Ionisation (ESI^+) at the DCM mass facility.

Synthesis

2,7-di-tert-butyl-4,9-di-(4-pyridyl)-*trans*-10b,10c-dimethyl-10b,10c-dihydropyrene (bis-pyridine-**DHP** ligand) was synthetized following our previously reported procedure.[32,40] *Cis*-[$PtCl_2(DMSO)_2$] was prepared using the method previously reported by Wayland and *coll.*[45]

Preparation of DHP-Pt$_2$

15.2 mg of *cis*-[$PtCl_2(DMSO)_2$] (36 μmol) were suspended in 2.5 mL of methanol and the mixture was refluxed until the complex was dissolved (~1h). 9 mg (18 μmol) of bis-pyridine-**DHP** ligand was then added and the solution was stirred at room temperature under dark conditions. After 12 hours, the resulting green-brown mixture was filtrated and the solid was washed with MeOH and Et_2O and dried under vacuum. If needed, **DHP-Pt$_2$** can be crystalized by dissolution in dichloromethane flowed by slow diffusion of Et_2O. yield: 72% (15.5 mg).

^{1}H NMR (400 MHz, 298 K, CD_2Cl_2) δ (ppm): -3.65 (s, 6H, int. CH_3), 1.68 (s, 18H, tBu), 3.54 (s, 12H, -CH_3 DMSO), 8.01 (m, 4H), 8.58 (s, 2H), 8.75 (m, 4H), 9.00 (m, 4H). ^{13}C NMR (125 MHz, $CDCl_3$) δ (ppm): 154.0, 151.6, 149.0, 137.4, 133.3, 130.1, 127.5, 124.8, 123.6, 120.2, 76.9, 51.1, 44.5, 36.6, 31.8, 30.5, 15.1. ESIMS: m/z: calcd for $C_{40}H_{50}Cl_4N_2O_2Pt_2S_2$: 1184.1 found: 1184.1.

Preparation of CPDO$_2$-Pt$_2$

CPDO$_2$-Pt$_2$ was prepared by *in situ* illumination of a solutions of **DHP-Pt$_2$**, as reported below (see section "Irradiation procedures"). The compound can be isolated as a yellow powder upon evaporation of the solvent at low temperature (<10°C) and can be stored for months at 4°C.

^{1}H NMR (400 MHz, CD_2Cl_2) δ (ppm): 0.00 (s, 3H), 1.09 (s, 9H), 1,28 (s, 9H), 2.10 (s, 3H), 3.47 (s, 6H), 3.49 (s, 6H), 6.79 (s, 1H); 6.98 (s, 1H), 7.06 (m, 1H), 7.29 (m, 2H), 7.38 (s, 1H), 7.52 (m, 2H), 7.63 (m, 2H), 8.70 (m, 2H), 8.77 (m, 2H). ESIMS: m/z: calcd for $C_{40}H_{50}Cl_4N_2O_4Pt_2S_2Na$: 1239.2 [$M+Na^+$] found: 1239.1.

X-Ray diffraction

Data for single crystal X-Ray diffraction were collected at 200 K on a Bruker AXS Enraf-Nonius Kappa APEXII diffractometer using the Mo-Kα monochromated radiation. Intensity data were collected for Lorentz and polarization effects and absorption with the EVAL14 software. Structures solutions and refinements were performed with the SHELX softwares implemented by Olex2. All non-hydrogen were refined by full matrix least-squares with anisotropic thermal parameters. Hydrogen atoms were introduced at calculated positions as riding atoms. Crystallographic structure of **DHP-Pt$_2$** was drawn with the Mercury 2022.3.0 software. CCDC-2240890 contains the supplementary crystallographic data for this paper. These data can be obtained free of charge from The Cambridge Crystallographic Data Centre via www.ccdc.cam.ac.uk/data_request/cif.

Spectroscopy

Absorption spectra were recorded using a Varian Cary 60 Scan UV/visible spectrophotometer equipped with a temperature controller unit. Absorption measurements over the spectral range from 250 to 800 nm were carried out in Hellma quartz suprasil cells (QS) having an optical path length of 1 cm. Emission spectra were recorded in CH_2Cl_2 at room temperature on a Varian Cary Eclipse fluorescence spectrophotometer.

Irradiation procedures

The solutions of **DHP-Pt$_2$** were irradiated in UV-visible quartz cells, NMR tubes or flasks under air (P = 1 atm.). Typically, concentrations used for UV-visible spectroscopy and NMR experiments were 2.10^{-5} M and 2 mg.mL^{-1} respectively. The visible irradiations for making the reaction from **DHP-Pt$_2$** to its corresponding endoperoxide form **CPDO$_2$-Pt$_2$** were carried out at room temperature either with a Xe-Hg lamp (500W) using a 630 nm cut-off filter or with mounted LEDs from Thorlab (M660L4, FWHM = 20 nm, 940-1050 mW), in combination of a Thorlab DC2200 led driver and an adjustable collimation adapter (SM2F32-A). The conversion reaction between the two forms was investigated from UV-visible and NMR experiments. Intermediate spectra were recorded at different times depending on the isomerization process rate.

Singlet oxygen production (Φ_Δ)

Singlet oxygen production quantum yields Φ_Δ were determined by the measure of the phosphorescence of singlet oxygen at λ = 1270 nm[51] with an Edinburgh Instruments FLS1000 fluorimeter equipped with an InGaAs detector. Experimentations were achieved at room temperature, with an oxygen non-saturated atmosphere (P = 1 atm).[52,53] Typically, solutions at 10^{-5} M in dichloromethane were prepared. Note that the reference and the sample have to be prepared in the same solvents in order to avoid singlet oxygen lifetimes deviation. Reference and sample were excited at a wavelength where they both have an optical density lower than 0.1. Excitation wavelength has to be preferentially in a zone where reference and sample have same absorbance tendency in order to reduce measurements uncertainty. Phenalenone photosensitizer was used as reference since it has high quantum yields near to the unity ($\Phi_\Delta \geq 0.94$) and it is soluble in a wide variety of solvents.[54] Φ_Δ was determined according to the following equation:

$$\Phi_\Delta^s = \Phi_\Delta^{ref} \times \frac{I_{\lambda^{ex}}^s A_{\lambda^{ex}}^{ref} \eta_s^2}{I_{\lambda^{ex}}^{ref} A_{\lambda^{ex}}^s \eta_{ref}^2} = \Phi_\Delta^{ref} \times \frac{I_{\lambda^{ex}}^s A_{\lambda^{ex}}^{ref}}{I_{\lambda^{ex}}^{ref} A_{\lambda^{ex}}^s} = \Phi_\Delta^{ref} \times \frac{S_{\lambda^{ex}}^s}{S_{\lambda^{ex}}^{ref}}$$

Where Φ_Δ^s and Φ_Δ^{ref} are singlet oxygen production quantum yields for sample and reference respectively. Reported singlet oxygen production quantum yield for phenalenone in dichloromethane is $\Phi_{\Delta_{CH2Cl2}}^{ref} = 0.98 \pm 0.08$. η_s and η_{ref} are the refractive index of the solvents. $\eta_s = \eta_{ref}$ as we work in the same solvents. $I_{\lambda^{ex}}^s$ and $I_{\lambda^{ex}}^{ref}$ are the integrated weak near-infrared phosphorescence of $^1O_2$ at λ = 1270 nm for the sample and the reference. This emission is characteristic of the deexcitation of the metastable singlet oxygen to its triplet ground state. The integrals were computed using an absolute integration by mathematical trapezoid sum algorithm implemented in Origin 9.5.0 software package.[55] $A_{\lambda^{ex}}^s$ and $A_{\lambda^{ex}}^{ref}$ denote for the absorbance of the sample and of the reference at the excitation wavelength λ^{ex}. $S_{\lambda^{ex}}^s$ and $S_{\lambda^{ex}}^{ref}$ stand for the slope of the line of the function $f(A_{\lambda^{ex}}) = I_{\lambda^{ex}}$ for the sample and the reference respectively meaning that $S_{\lambda^{ex}}^s = I_{\lambda^{ex}}^s / A_{\lambda^{ex}}^s$ and $S_{\lambda^{ex}}^{ref} = I_{\lambda^{ex}}^{ref} / A_{\lambda^{ex}}^{ref}$. By plotting the function $f(A_{\lambda^{ex}}) = I_{\lambda^{ex}}$ for at least 5 different concentrations, $S_{\lambda^{ex}}^s$ and $S_{\lambda^{ex}}^{ref}$ can be determined as the slopes of the lines.

Confocal microscopy

The z-stack images of cell-cultures were captured using a TCS SP8 GSU Leica (HC PL APO CS2, 40X/1.30 OIL, zoom 3.2, with a z voxel size = 0.569 µm and an image resolution of 1024 x 1024 pixels. H_2DCFDA probe: Excitation wavelength was 488 nm and emission was collected in the 500 - 550 nm range. Hoechst 33342: Excitation: λ = 405 nm and fluorescence emission collected between λ = 450 and 500 nm. **DHP-Pt$_2$** or **CPDO$_2$-Pt$_2$**: Excitation at λ = 405 nm and fluorescence emission collected between λ = 650 and 750 nm. Images were processed using ImageJ software.[56] The solution-absorbance in microplates was read on a POLARstar Omega plate reader (BMG labtech).

Cell lines and culture conditions

BT-549 (human breast ductal carcinoma), HeLa (human cervical carcinoma), A-549 (human lung adenocarcinoma) and A-375 (human melanoma) cell lines were obtained from the American Type Culture Collection (ATCC, Manassas, VA, USA). BT-549 , A-549 and A-375 cell lines were cultured in RPMI-1640 medium supplemented with 10% FBS, 1% penicillin and streptomycin in a humidified 5% CO_2 incubator at 37°C. HeLa and HFF-1 cells were grown in DMEM supplemented with 10% FBS, 1% penicillin and streptomycin at 37°C under 5% CO_2 atmosphere.

Interaction with DNA plasmid

Gel-electrophoretic mobility shift assay is commonly used to study the interaction via intercalation or covalent crosslinking of metallic complexes with double helix DNA. Stock solutions of platinum (II) compounds were prepared in 10 mM phosphate buffer, pH 7.5, 10% DMSO. pBR322 plasmid DNA aliquots (13 µg.mL^{-1} in 10 mM phosphate buffer, pH 7.5 containing 10% DMSO) were incubated with increasing concentrations of platinum complexes ranging from 0.09 to 25 µM at 37°C for 16h in the dark (**CPDO$_2$-Pt$_2$** was freshly preformed before incubation with DNA by illumination of a solution of **DHP-Pt$_2$** as previously described). DNA loading buffer was then added to the samples and the

resulting mixtures containing complexes-DNA products were loaded onto 1% agarose gel in tris-Boric-EDTA buffer (pH 8.2) (0.5 x TBE). Electrophoresis was performed at 70 V for 2h. After DNA migration, the gels were stained in the same buffer containing ethidium bromide (0.5 mg.mL^{-1}) and visualised using Molecular Imager, Gel DocTM XR and image LabTM Software.

Intracellular singlet oxygen release

DCFH-DA was used as $^1O_2$ probe. Cells (1.10^5 cells.mL^{-1}) were seeded in Lab-Tek chamber slides and allowed to grow for 24h. Compounds (**DHP-Pt$_2$** or **CPDO$_2$-Pt$_2$**) were directly added in the cell culture (10 μM final concentration) and the incubation was continued for 24h at 37°C, 5% CO_2. Culture medium was then removed and cells were treated with DCFH-DA (4 μM in PBS) for another 0.5 h at 37°C. In parallel, cells without compound treatment were incubated with DCFH-DA and used as control. Cells were then washed with PBS and confocal fluorescence imaging was used to image intracellular singlet oxygen delivery.

Cell viability assay

Cytotoxicity of platinum complexes (**DHP-Pt$_2$** or **CPDO$_2$-Pt$_2$**) and cisplatin used as reference were measured using MTT assay as previously described.[57] Cells were seeded in 96-well plates (4.10^3 cells.well^{-1} for A-549 and A-375, 1.10^4 cells.well^{-1} for HeLa and 2.10^4 cells.well^{-1} for BT-549) and allowed to attach for overnight. Cells were then treated with 50 μM of each compound for 48h for single concentration assay or with a range concentration of 0.78 to 100 μM for 24h, 48h and 72h for dose-response curves. MTT solution (0.5 mg.mL^{-1} in culture media) was added to each well and the cells were further incubated at 37°C for 4h. Subsequently, the media was removed and the blue formazan crystals were dissolved in 100 μL of DMSO. The absorbance value was measured at 570 nm with a microplate reader and the cell viability was calculated using the following formula:

$$Cell\ viability\ (\%) = \left(\frac{OD_{Sample} - OD_{Blank}}{OD_{Control} - OD_{Blank}}\right) \times 100$$

Confocal microscopy for cell-compound localization

Cells were seeded onto coverslips in 8-wells labtek with a cell density of 4.10^4 cells.well^{-1} and allowed to attach for 24h. Complexes (25 μM) or blank PBS were added and cells were incubated at 37°C in a humidified 5% CO_2 incubator for 24 h. The medium was then removed and cells were washed with PBS before to be fixed for 10 min at 4°C in 4% paraformaldehyde (PFA) solution. Cell nucleus were then stained with Hoechst 33342 (1 μM) for 20 min at room temperature. After washing with PBS, cells were imaged with confocal microscope.